NASA Technical Memorandum 78605

Flux Vector Splitting of the Inviscid Gasdynamic Equations With Application to Finite Difference Methods

Joseph L. Steger and R. F. Warming

(NASA-TM-78605) FLUX VECTOR SPLITTING OF THE INVISCID EQUATIONS WITH APPLICATION TO FINITE DIFFERENCE METHODS (NASA) 54 p
HC A04/MF A01 CSCL 12A G3/64

N79-28950

Unclas
29419

July 1979

National Aeronautics and Space Administration

NASA Technical Memorandum 78605

Flux Vector Splitting of the Inviscid Gasdynamic Equations With Application to Finite Difference Methods

Joseph L. Steger
R. F. Warming, Ames Research Center, Moffett Field, California

NASA
National Aeronautics and
Space Administration

Ames Research Center
Moffett Field, California 94035

CONTENTS

LIST OF SYMBOLS

Roman Lower Case

c

e

f

i

j

k

m

n

p

t

u

v

w

x

y

Roman Upper Case

A

B

F

G

I

J

M

P

Q

Roman Upper Case (continued)

T

U

Greek Lower Case

α

β

γ

$\delta_x,\ \delta_x^B,\ \delta_x^F$

ϵ

η

θ

λ

ν

ξ

ρ

σ

τ

Greek Upper Case

Λ

Script Upper Case

$\mathscr{F}_I,\ \mathscr{F}_{II}$

Script Lower Case

ℓ

SUMMARY

The conservation-law form of the inviscid gasdynamic equations has the remarkable property that the nonlinear flux vectors are homogeneous functions of degree one. This property readily permits the splitting of flux vectors into subvectors by similarity transformations so that each subvector has associated with it a specified eigenvalue spectrum. As a consequence of flux vector splitting, new explicit and implicit dissipative finite-difference schemes are developed for first-order hyperbolic systems of equations. Appropriate one-sided spatial differences for each split flux vector are used throughout the computational field even if the flow is locally subsonic. The results of some preliminary numerical computations are included.

1. INTRODUCTION

Finite-difference schemes for the conservation-law form of the unsteady inviscid gasdynamic equations are restricted to a very limited class of spatial difference approximations in subsonic flow regions. Only centered difference operators lead to difference methods that are simultaneously stable for both the positive and negative characteristic speeds (i.e., eigenvalues) that are associated with the spatial flux terms in subsonic flow. Use of any other class of spatial differential operator requires splitting the flux terms into components of a restricted type.

There are various reasons for using one-sided spatial difference operators. For example, for the model scalar wave equation, one-sided (or upwind) schemes frequently have superior dissipation and dispersive properties to those of a centered scheme [1,2]. An explicit second-order accurate upwind scheme can also have twice the stability bound of a centered second-order scheme [1]. Another motivation stems from a desire to increase numerical efficiency of implicit algorithms. For example, an implicit upwind finite difference algorithm can lead to a lower diagonal banded matrix that is more easily inverted than the tridiagonal and pentadiagonal matrices usually associated with centered schemes.

Our objective is to devise a means of splitting the flux vectors of a hyperbolic system in order to extend the class of allowable spatial differencing schemes to achieve more robust

algorithms and to improve computational efficiency. As in earlier related work [2,3], we restrict our attention to the inviscid gasdynamic equations in conservation-law form and take advantage of the fact that the flux vectors are homogeneous of degree one. We have not investigated first-order conservative systems that are nonhomogeneous. The basic ideas used here, however, apply to first-order nonconservative hyperbolic systems of equations. A related explicit algorithm for the equations of gasdynamics written in nonconservation law form was recently proposed by Moretti [4].

In this paper we first review the restrictions placed on the spatial difference operators of hyperbolic systems that have both positive and negative eigenvalues. Using the one-dimensional inviscid equations of gasdynamics, we then develop a methodology for splitting the equations into components of the same characteristic behavior. Both explicit and implicit numerical algorithms are devised and tested for the split system of equations. The methodology and algorithms are then extended to multidimensions.

2. MOTIVATION AND BACKGROUND

In this section we review the restrictions placed on spatial difference approximations by the characteristic speeds (eigenvalues) of a hyperbolic system.

To illustrate the basic notions we consider a one-dimensional system of conservation laws

$$\frac{\partial U}{\partial t} + \frac{\partial F}{\partial x} = 0 \ , \tag{2.1}$$

where U and F are m-component column vectors. The system (2.1) can be rewritten as a quasi-linear system

$$\frac{\partial U}{\partial t} + A(U) \frac{\partial U}{\partial x} = 0 \ , \tag{2.2}$$

where A is the Jacobian matrix $\partial F/\partial U$. The system (2.2) is hyperbolic at the point (x,t,U) if there exists a similarity transformation such that

$$Q^{-1}AQ = \Lambda = \begin{bmatrix} \lambda_1 & & & & \\ & \lambda_2 & & \mathbf{0} & \\ & & \lambda_3 & & \\ & & & \ddots & \\ \mathbf{0} & & & & \lambda_m \end{bmatrix} \tag{2.3}$$

where Λ is a diagonal matrix, the eigenvalues λ_ℓ of A are real, and the norms of Q and Q^{-1} are uniformly bounded.

For the purpose of a linear stability analysis, we assume that the coefficient matrix A is "frozen," that is, constant. By virtue of Eq. (2.3), Eq. (2.2) can be transformed to the uncoupled system

$$\frac{\partial u_\ell}{\partial t} + \lambda_\ell \frac{\partial u_\ell}{\partial x} = 0 \ , \qquad \ell = 1, 2, 3, \ldots, m \tag{2.4}$$

by defining a new vector $u = (u_1, u_2, u_3, \ldots, u_m)^t = Q^{-1}U$. Consequently, when analyzing the stability of numerical algorithms as applied to the linearized version of the system (2.2), we need only examine the scalar Eq. (2.4). For simplicity, the subscript ℓ will be dropped in the remainder of this section.

To analyze the effect of one-sided spatial differences on stability we leave the time variable continuous and discretize the spatial variable as $x = x_j = j\Delta x$. Let $\partial u/\partial x$ be approximated by the first-order one-sided difference quotient

$$\left.\frac{\partial u}{\partial x}\right|_j = \frac{\nabla_x u_j}{\Delta x} + O(\Delta x) , \tag{2.5}$$

where ∇_x is the classical backward-difference operator

$$\nabla_x u_j = u_j - u_{j-1} . \tag{2.6}$$

This spatial discretization reduces Eq. (2.4) to a system of first-order ordinary differential equations:

$$\frac{du_j}{dt} + \lambda \frac{u_j - u_{j-1}}{\Delta x} = 0 . \tag{2.7}$$

For simplicity, assume spatially periodic boundary conditions and look for a solution of the form

$$u_j(t) = v(t)e^{ikj\Delta x} , \tag{2.8}$$

where $v(t)$ is the Fourier coefficient, $i = \sqrt{-1}$, and k is the wave number. By inserting Eq. (2.8) in Eq. (2.7), one finds that the Fourier coefficient satisfies the ordinary differential equation

$$\frac{dv}{dt} = \sigma v , \tag{2.9a}$$

where

$$\sigma = -\frac{\lambda}{\Delta x}\left[2 \sin^2\left(\frac{\theta}{2}\right) + i \sin\theta\right] , \qquad \theta = k\Delta x . \tag{2.9b}$$

The solution is $v = Ce^{\sigma t}$ so for Eq. (2.9a) to have a bounded solution, the real part of σ must satisfy $\mathrm{Re}\,\sigma \le 0$, which requires that $\lambda > 0$.

Instead of the backward-difference operator (2.6), let $\partial u/\partial x$ be approximated by

$$\left.\frac{\partial u}{\partial x}\right|_j = \frac{1}{\Delta x}\Delta_x u_j + O(\Delta x) , \tag{2.10}$$

where Δ_x is the forward-difference operator

$$\Delta_x u_j = u_{j+1} - u_j . \tag{2.11}$$

If we repeat the Fourier stability analysis, we find

$$\sigma = \frac{\lambda}{\Delta x}\left[2\sin^2\left(\frac{\theta}{2}\right) - i\sin\theta\right] , \qquad \theta = k\Delta x . \tag{2.12}$$

Again, for stability, $\mathrm{Re}\sigma \le 0$, and we now require that $\lambda < 0$.

In summary, for one-sided spatial difference approximations we have the following result: If $\partial u/\partial x$ is approximated by the backward-difference operator (2.6), then the resulting ordinary differential equation (2.7) will be stable if and only if $\lambda > 0$ (i.e., the wave travels to the right). Conversely, if $\partial u/\partial x$ is approximated by the forward-difference operator (2.11), the resulting ordinary differential equation (2.7) will be stable if and only if $\lambda < 0$ (i.e., the wave travels to the left). In general, no conventional backward, forward, or unsymmetric operator such as

$$\left.\frac{\partial u}{\partial x}\right|_j = \frac{-2u_{j-1} - 3u_j + 6u_{j+1} - u_{j+2}}{6\Delta x} + O(\Delta x^3) \tag{2.13}$$

will yield an ordinary differential equation which is simultaneously stable for both positive and negative eigenvalues. Although this statement is justified in Appendix A, its correctness is apparent from the fact that any noncentered spatial-difference operator will yield an eigenvalue (see, e.g., Eq. (2.9b)) with a nonzero real part whose coefficient is the eigenvalue λ. Hence, the real part cannot satisfy $\mathrm{Re}\sigma < 0$ for both positive and negative λ.

Returning to the system (2.1), it is clear that if a single noncentered difference operator is used to approximate $\partial F/\partial x$ when the eigenvalues of the Jacobian matrix A are of mixed sign, then the resulting time-continuous method will always produce a numerical instability.

3. ONE-DIMENSIONAL EQUATIONS OF GASDYNAMICS

In one spatial dimension the inviscid equations of gasdynamics can be written in the conservation-law form (2.1) where

$$U = \begin{bmatrix} \rho \\ m \\ e \end{bmatrix} \qquad F(U) = \begin{bmatrix} m \\ (m^2/\rho) + p \\ (e + p)m/\rho \end{bmatrix}, \tag{3.1a,b}$$

and where $m = \rho u$. The primitive variables of (3.1) are the density ρ, the velocity u, and the pressure p. The total energy per unit volume, e, is related to the internal energy per unit mass, ε, by

$$e = \rho\varepsilon + \rho u^2/2 = \rho\varepsilon + m^2/(2\rho) . \tag{3.2}$$

The system is completed with an equation of state

$$p = p(\rho,\varepsilon) \ . \tag{3.3}$$

For the case of a perfect gas,

$$p = (\gamma - 1)\rho\varepsilon \ , \tag{3.4}$$

which can be rewritten using (3.2) as

$$p = (\gamma - 1)[e - m^2/(2\rho)] \ , \tag{3.5}$$

where γ is the ratio of specific heats.

By using (3.5), the flux vector $F(U)$ can be rewritten as

$$F(U) = \begin{bmatrix} m \\ (\gamma - 1)e + (3 - \gamma)m^2/(2\rho) \\ \gamma em/\rho - (\gamma - 1)m^3/(2\rho^2) \end{bmatrix} \ . \tag{3.6}$$

The Jacobian matrix $A = \partial F/\partial U$ is easily computed and found to be

$$A = \begin{bmatrix} 0 & 1 & 0 \\ (\gamma - 3)u^2/2 & (3-\gamma)u & \gamma - 1 \\ (\gamma - 1)u^3 - \gamma eu/\rho & \gamma e/\rho - 3(\gamma - 1)u^2/2 & \gamma u \end{bmatrix} . \tag{3.7}$$

The eigenvalues of A are

$$\lambda_1 = u \ , \quad \lambda_2 = u + c \ , \quad \lambda_3 = u - c \ , \tag{3.8}$$

where $c = (\gamma p/\rho)^{1/2}$ is the local speed of sound. For subsonic flow $|u| < c$, and the eigenvalues are of mixed sign since $u + c$ and $u - c$ are of opposite sign.

The inviscid equations of gasdynamics have the rather remarkable property that if the equation of state has the functional form

$$p = \rho f(\varepsilon) \ , \tag{3.9}$$

then the nonlinear flux vector $F(U)$ is a homogeneous function of degree one in U; that is $F(\alpha U) = \alpha F(U)$ for any value α. The equation of state (3.4) is clearly a special case of (3.9) and the fact that $F(U)$ is a homogeneous function of degree one is obvious by inspection of the flux vector (3.6). By application of Euler's theorem on homogeneous functions (see, e.g., [5]) there follows

$$F = AU \ , \tag{3.10}$$

where A is the Jacobian matrix $\partial F/\partial U$. One can readily verify the above equality by using Eqs. (3.7) and (3.1a) and making the indicated matrix-vector multiply. The flux vectors in two and three spatial dimensions also have the homogeneous property.

If F satisfies the homogeneous property and A has a complete set of linearly independent eigenvectors, then the flux vector F can be split into subvectors, each one of which is associated with a tailored set of eigenvalues. In particular, the eigenvalues associated with one subvector can be all positive, those associated with the other all negative. These subvectors can then be differenced individually with an appropriate one-sided scheme in conservation-law form. The details for the one-dimensional case are outlined in the following section.

4. FLUX VECTOR SPLITTING FOR THE ONE-DIMENSIONAL EQUATIONS OF GASDYNAMICS

Consider Eq. (2.1) with U and F defined by Eq. (3.1). The flux vector $F(U)$ has the homogeneous property defined in the preceding section and consequently F can be split into two parts as [2], [3]

$$F = F^+ + F^- , \tag{4.1}$$

where F^+ corresponds to the subvector associated with the positive eigenvalues of A, and F^- corresponds to the negative eigenvalues. This splitting is derived as follows. By virtue of (3.10) and (2.3),

$$F = AU = Q\Lambda Q^{-1}U , \tag{4.2}$$

where the diagonal elements of Λ are given by (3.8).

Any eigenvalue λ_ℓ can be expressed as

$$\lambda_\ell = \lambda_\ell^+ + \lambda_\ell^- , \tag{4.3}$$

where

$$\lambda_\ell^+ = \frac{\lambda_\ell + |\lambda_\ell|}{2} , \qquad \lambda_\ell^- = \frac{\lambda_\ell - |\lambda_\ell|}{2} , \tag{4.4}$$

so that if $\lambda_\ell \geq 0$ then $\lambda_\ell^+ = \lambda_\ell$, $\lambda_\ell^- = 0$, with the converse result for $\lambda_\ell < 0$.

Using the above formulas, we split the diagonal matrix

$$\Lambda = \Lambda^+ + \Lambda^- , \tag{4.5}$$

where Λ^+ and Λ^- have as diagonal elements λ_ℓ^+ and λ_ℓ^-, respectively. Equation (4.2) can be rewritten as

$$F = Q(\Lambda^+ + \Lambda^-)Q^{-1}U$$
$$= (A^+ + A^-)U$$
$$= F^+ + F^- , \qquad (4.6)$$

where

$$A^+ = Q\Lambda^+Q^{-1} , \qquad A^- = Q\Lambda^-Q^{-1} \qquad (4.7)$$

$$F^+ = A^+U , \qquad F^- = A^-U , \qquad (4.8)$$

and

$$A = A^+ + A^- . \qquad (4.9)$$

The eigenvalues of A^+ are nonnegative and those of A^- are nonpositive. For the inviscid gasdynamic equations, the matrices Q and Q^{-1} are given by

$$Q = MT , \qquad Q^{-1} = T^{-1}M^{-1} , \qquad (4.10)$$

where M and T and their inverses are given in [2] for one and two space dimensions and in [6] for three space dimensions.

The eigenvalues given by Eqs. (3.8) are split according to Eqs. (4.3) and (4.4) into

$$\left.\begin{aligned} \lambda_1^+ &= \frac{u + |u|}{2} & \lambda_1^- &= \frac{u - |u|}{2} \\ \lambda_2^+ &= \frac{u + c + |u + c|}{2} & \lambda_2^- &= \frac{u + c - |u + c|}{2} \\ \lambda_3^+ &= \frac{u - c + |u - c|}{2} & \lambda_3^- &= \frac{u - c - |u - c|}{2} . \end{aligned}\right\} \qquad (4.11)$$

The corresponding subvectors F^+ and F^- for the special case $0 \le u \le c$ are

$$F^+ = \frac{\rho}{2\gamma}\begin{bmatrix} 2\gamma u + c - u \\ 2(\gamma-1)u^2 + (u+c)^2 \\ (\gamma-1)u^3 + \frac{(u+c)^3}{2} + \frac{(3-\gamma)(u+c)c^2}{2(\gamma-1)} \end{bmatrix},$$

$$F^- = \frac{\rho}{2\gamma}\begin{bmatrix} u - c \\ (u-c)^2 \\ \frac{(u-c)^3}{2} + \frac{(3-\gamma)(u-c)c^2}{2(\gamma-1)} \end{bmatrix}, \qquad (4.12a)$$

or, if $u > c$,

$$F^+ = F\ , \qquad F^- = 0\ , \qquad (4.12b)$$

where F is (3.6). The subvectors (4.12a) can be obtained, by a tedious calculation, directly from (4.6) or from the generalized flux vector (4.19) given at the end of this section.

The eigenvalue splitting (4.4) is not unique and other splittings into positive and negative parts are possible. For example, consider the splitting given by [3]:

$$\left.\begin{aligned} \lambda_1^+ &= \frac{u + |u|}{2} & \lambda_1^- &= \frac{u - |u|}{2}\ , \\ \lambda_2^+ &= \lambda_1^+ + c & \lambda_2^- &= \lambda_1^-\ , \\ \lambda_3^+ &= \lambda_1^+ & \lambda_3^- &= \lambda_1^- - c\ , \end{aligned}\right\} \qquad (4.13)$$

which satisfies (4.3) and the sum $\lambda_\ell^+ + \lambda_\ell^- = \lambda_\ell$ gives the physical eigenvalues.

A more general class of splitting is given by

$$\lambda_\ell = \lambda_\ell^\alpha + \lambda_\ell^\beta + \ldots\ , \qquad (4.14)$$

with corresponding subvectors

$$F = F^{\alpha} + F^{\beta} + \ldots , \tag{4.15}$$

where λ_{ℓ} is not necessarily split into positive and negative parts. For example, the sound wave or pressure term contribution to the eigenvalue could be split from the flow velocity. In the general notation (4.15) with $\alpha = u$ and $\beta = c$, one has

$$\left.\begin{aligned} \lambda_1^u &= u \quad & \lambda_1^c &= 0 , \\ \lambda_2^u &= u \quad & \lambda_2^c &= c , \\ \lambda_3^u &= u \quad & \lambda_3^c &= -c , \end{aligned}\right\} \tag{4.16}$$

and the subvectors are given by

$$F^u = uU = u \begin{bmatrix} \rho \\ m \\ e \end{bmatrix} , \qquad F^c = \begin{bmatrix} 0 \\ p \\ up \end{bmatrix} . \tag{4.17}$$

This splitting, in two and three dimensions, has been used in parabolized Navier-Stokes calculations [7].

Since several splittings are possible, it is convenient to define a "generalized" flux vector from which any split subvector can readily be computed. The generalized flux vector is defined by

$$\mathcal{F}_I = Q\hat{\Lambda}Q^{-1}U , \tag{4.18}$$

where $\hat{\Lambda}$ is the diagonal matrix

$$\hat{\Lambda} = \begin{bmatrix} \hat{\lambda}_1 & & 0 \\ & \hat{\lambda}_2 & \\ 0 & & \hat{\lambda}_3 \end{bmatrix}$$

whose eigenvalues $\hat{\lambda}_\ell$ are arbitrary. A direct calculation for the one-dimensional gasdynamic equations yields

$$\mathscr{F}_I = \frac{\rho}{2\gamma} \begin{bmatrix} 2(\gamma - 1)\hat{\lambda}_1 + \hat{\lambda}_2 + \hat{\lambda}_3 \\ 2(\gamma - 1)\hat{\lambda}_1 u + \hat{\lambda}_2(u+c) + \hat{\lambda}_3(u-c) \\ (\gamma - 1)\hat{\lambda}_1 u^2 + \frac{\hat{\lambda}_2}{2}(u+c)^2 + \frac{\hat{\lambda}_3}{2}(u-c)^2 + w \end{bmatrix}, \quad (4.19)$$

where

$$w = \frac{(3 - \gamma)(\hat{\lambda}_2 + \hat{\lambda}_3)c^2}{2(\gamma - 1)} \quad . \quad (4.20)$$

The vector $\mathscr{F}_I$ has a rather striking structure. One can easily verify that if the $\hat{\lambda}_\ell$ are replaced by the physical eigenvalues (3.8), then (4.19) reduces to the physical flux vector (3.6) which, of course, must follow by Eq. (4.2). Flux formulas for any splitting follow directly by inserting the appropriate split eigenvalues (4.14) into Eq. (4.19). In particular, to arrive at the splitting defined by Eq. (4.11), F^+ follows directly by inserting λ_ℓ^+ into Eq. (4.19), and F^- follows by inserting λ_ℓ^- into Eq. (4.19). The matrices A^+ and A^- can be obtained from Eq. (4.7). The other splittings are obtained in a similar way.

The generalized flux vectors $\mathscr{F}_{II}$, $\mathscr{F}_{III}$ for two and three spatial dimensions are given in Appendix B. From these generalized vectors, the flux vectors for any eigenvalue splitting can easily be computed for the inviscid equations of gasdynamics.

In concluding this section we remark that, in general, $A^+ \neq \partial F^+/\partial U$ and $A^- \neq \partial F^-/\partial U$. However, in all the numerical tests

that we have made, $\partial F^+/\partial U$ does have positive eigenvalues and $\partial F^-/\partial U$ has negative eigenvalues; these roots, however, are not identical to those of A^+ and A^-.

5. ALGORITHMS FOR ONE SPACE DIMENSION

In this section we illustrate several numerical algorithms that can be constructed for the one-dimensional equations of gas-dynamics by use of flux vector splitting.

Explicit Methods

MacCormack's scheme [8] for the one-dimensional system of conservation laws (2.1) is

$$\overline{U_j^{n+1}} = U_j^n - \Delta t \frac{\nabla_x F_j^n}{\Delta x} , \tag{5.1}$$

$$U_j^{n+1} = \frac{1}{2} (\overline{U_j^{n+1}} + U_j^n) - \frac{\Delta t}{2} \frac{\Delta_x \overline{F_j^{n+1}}}{\Delta x} , \tag{5.2}$$

where U_j^n denotes the finite-difference approximation to U, $F_j^n = F(U_j^n)$, etc., and the forward and backward difference operators are defined by Eqs. (2.11) and (2.6).

Since the predictor (5.1) is one-sided (upwind), the corrector (5.2) can be modified as

$$U_j^{n+1} = \frac{1}{2} (U_j^n + \overline{U_j^{n+1}}) - \frac{\Delta t}{2} \frac{\nabla_x^2 F_j^n}{\Delta x} - \frac{\Delta t}{2} \frac{\nabla_x \overline{F^{n+1}}}{\Delta x} , \tag{5.3}$$

to obtain a completely upwind second-order scheme [1]. A necessary local condition for the stability of the scheme Eqs. (5.1) and (5.3) is that all the eigenvalues of the Jacobian matrix A be positive.

MacCormack's scheme can be modified by using a forward difference in the predictor, and a backward difference in the corrector. Likewise, the upwind scheme (5.1), (5.3) can be altered by replacing ∇ by Δ and ∇^2 by $-\Delta^2$. In this case a necessary condition for the stability of the altered scheme is that all the eigenvalues of the Jacobian matrix be negative.

The eigenvalue splitting (4.11) or (4.13) of the previous section can be used so that a split upwind version of MacCormack's scheme can be used when the eigenvalues are of mixed sign, that is, in a subsonic region. The split upwind algorithm is

$$\overline{U_j^{n+1}} = U_j^n - \Delta t \frac{\nabla_x (F_j^+)^n}{\Delta x} - \Delta t \frac{\Delta_x (F_j^-)^n}{\Delta x}, \tag{5.4}$$

$$U_j^{n+1} = \frac{1}{2}\left(U_j^n + \overline{U_j^{n+1}}\right) - \frac{\Delta t}{2}\left(\frac{\nabla_x^2 (F_j^+)^n}{\Delta x} + \frac{\nabla_x (F_j^+)^{\overline{n+1}}}{\Delta x}\right)$$
$$+ \frac{\Delta t}{2}\left(\frac{\Delta_x^2 (F_j^-)^n}{\Delta x} - \frac{\Delta_x (F_j^-)^{\overline{n+1}}}{\Delta x}\right). \tag{5.5}$$

According to linear stability theory, the scheme (5.4) and (5.5) is stable if and only if

$$|\lambda_\ell^\pm| \Delta t/\Delta x \leq 2$$

for all eigenvalues $\lambda_\ell^\pm$ where $\lambda_\ell = \lambda_\ell^+ + \lambda_\ell^-$ are the eigenvalues of the Jacobian matrix.

The MacCormack scheme, (5.1) and (5.2), is a symmetric scheme in the sense that the grid point cluster is symmetric about the center point j at the completion of the corrector step. A symmetric (explicit) second-order scheme has a predominantly lagging

phase error and an upwind scheme has a leading phase error [1]. The opposite phase error of the symmetric and the upwind schemes suggests that a considerable reduction of phase error would occur if the two schemes were alternated on successive time steps. A temporal switching of schemes is the basis of Fromm's method of zero-average phase error [9].

Implicit Methods

A noniterative implicit finite-difference scheme, for a one-dimensional system of conservation laws is [2]

$$\left(I + \frac{\theta\Delta t}{1+\xi}\,\delta_x A_j^n\right)\Delta U_j^n = -\frac{\Delta t}{1+\xi}\,\delta_x F_j^n + \frac{\xi}{1+\xi}\,\Delta U_j^{n-1}\,, \qquad (5.6)$$

where I is the identity matrix, $\Delta U^n = U^{n+1} - U^n$, A is the Jacobian matrix, and δ_x is an appropriate spatial difference operator.* In general, the spatial derivative approximations on the left- and right-hand sides of (5.6) can be different. The parameters θ,ξ determine the particular time-differencing approximation used. Scheme (5.6) includes three well-known implicit formulas

$\theta = \frac{1}{2}$, $\xi = 0$ trapezoidal formula;

$\theta = 1$, $\xi = 0$ backward Euler;

$\theta = 1$, $\xi = \frac{1}{2}$ three-point backward.

For a more general formulation that includes all linear multistep (time-differencing) methods see [10].

*In Eq. (5.6) and in similar equations throughout this paper, notation of the form $(I + \Delta t\delta_x A)\Delta U$ denotes $\Delta U + \Delta t\delta_x(A\Delta U)$.

With use of the split flux vectors (4.7), one-sided spatial difference approximations are possible. For example,

$$\left[I + \frac{\theta\Delta t}{1+\xi}\left(\nabla_x A_j^+|^n + \Delta_x A_j^-|^n\right)\right]\Delta U_j^n$$

$$= -\left(\frac{\Delta t}{1+\xi}\right)\left(\delta_x^b F_j^+|^n + \delta_x^f F_j^-|^n\right) + \frac{\xi}{1+\xi}\Delta U_j^{n-1} \quad , \tag{5.7}$$

where

$$\delta_x^b F_j = \frac{3F_j - 4F_{j-1} + F_{j-2}}{2\Delta x} \tag{5.8}$$

and

$$\delta_x^f F_j = \frac{-3F_j + 4F_{j+1} - F_{j+2}}{2\Delta x} \tag{5.9}$$

are second-order accurate one-sided difference operators.

The splitting $F = F^+ + F^-$ allows an approximate factorization of the left-hand side of (5.7) into the product of two operators as

$$\left(I + \frac{\theta\Delta t}{1+\xi}\nabla_x A_j^+|^n\right)\left(I + \frac{\theta\Delta t}{1+\xi}\Delta_x A_j^-|^n\right)\Delta U_j^n$$

$$= -\left(\frac{\Delta t}{1+\xi}\right)\left(\delta_x^b F_j^+|^n + \delta_x^f F_j^-|^n\right) + \frac{\xi}{1+\xi}\Delta U_j^{n-1} \quad . \tag{5.10}$$

This scheme is implemented by the sequence

$$\left(I + \frac{\theta\Delta t}{1+\xi}\nabla_x A_j^+|^n\right)\Delta U_j^* = -\left(\frac{\Delta t}{1+\xi}\right)\left(\delta_x^b F_j^+|^n + \delta_x^f F_j^-|^n\right) + \frac{\xi}{1+\xi}\Delta U_j^{n-1} \quad , \tag{5.11a}$$

$$\left(I + \frac{\theta\Delta t}{1+\xi}\Delta_x A_j^-|^n\right)\Delta U_j^n = \Delta U_j^* \quad , \tag{5.11b}$$

$$U_j^{n+1} = U_j^n + \Delta U_j^n \quad . \tag{5.11c}$$

Unlike Eq. (5.7), the solution of Eq. (5.10) does not require the solution of a block tridiagonal system because both Eqs. (5.11a) and (5.11b) lead to block bidiagonal systems. For example, by writing out (5.11b)

$$\left[I - \frac{\theta}{1+\xi}\frac{\Delta t}{\Delta x}\,(A_j^-)^n\right]\Delta U_j^n = \Delta U_j^* - \frac{\theta}{1+\xi}\frac{\Delta t}{\Delta x}\,(A_{j+1}^-)^n \Delta U_{j+1}^n \,, \qquad (5.12)$$

we see that the solution is achieved by a right to left sweep (decreasing j) with the inversion of the 3×3 matrix in the parenthesis on the left required at each mesh point. The eigenvalues of this matrix are greater than or equal to unity and consequently the matrix is nonsingular for any Δt.

The scheme (5.10) is second-order accurate, dissipative, and unconditionally stable for $\theta = 1$, $\zeta = 1/2$ (according to linear theory). In one spatial dimension, computational efficiency can be lost in comparison to Eq. (5.6) with δ_x a three-point central operator. This is chiefly because A^+, A^-, F^+, and F^- are costly to form. In multidimensions, however, an advantage is achieved by avoiding the solution of block tridiagonal systems.

6. NUMERICAL EXPERIMENTS IN ONE DIMENSION

The numerical solution of a one-dimensional shock-tube flow was chosen to judge the viability of the numerical algorithms given in the previous section. As a model problem, consider a tube of large extent in which a diaphragm separates a perfect gas at rest with different static pressures but at a uniform temperature.

With rupture of the diaphragm, an expansion propagates into the high-pressure gas, while a shock wave, followed by a contact surface, propagates into the low-pressure gas. Details of this flow are described in standard texts (e.g., Liepmann and Roshko [11]).

In our calculations, the initial pressure ratio across the diaphragm is taken as 5 to 1. The solution results for various methods are shown in Figs. 1 to 5 in terms of the nondimensional density, ρ/ρ_0, where ρ_0 is the initial high-density gas. In all cases, the same spatial grid and time step are used and $\Delta t/\Delta x = 0.2$.

The results for the explicit upwind scheme (5.4), (5.5) are shown in Fig. 1. Also shown are the exact locations of the shock and contact waves and exact constant density levels. The initial location of the diaphragm is taken at $x = 3.0$. Overall, the numerical accuracy is good and although the contact wave is smoothed out, the overshoots are moderate. For comparison purposes, the results for this flow obtained using the conventional MacCormack scheme are shown in Fig. 2. The accuracy of the two schemes is comparable, with the exception of a large spike in density as a result of start up. MacCormack has shown that the addition of a dissipation term, especially in expansion regions, can control such spikes [12]. We did not program this version, however, in order to illustrate the effectiveness of alternating the centered and upwind schemes.

In Fig. 3 we show the solution obtained using the upwind scheme (5.4), (5.5) to advance the solution for odd values of the time index n and using the MacCormack scheme (5.1), (5.2) for the even values of n. The results of this combined algorithm are clearly superior to the application of either of its constituents. The overshoots are much reduced, and the jumps are crisper.

Results for the implicit upwind scheme (5.10), are shown in Fig. 4. Here, trapezoidal time-differencing was used. Again the results are good and quite comparable to those obtained with the explicit procedure. Finally, in Fig. 5 we show the results obtained from the "conventional" implicit algorithm using centered spatial differencing and three-point backward time-differencing. A small amount of fourth-order numerical dissipation was also added [13]. Overall, the results are again quite comparable.

7. FLUX VECTOR SPLITTING IN TWO SPACE DIMENSIONS

In two spatial dimensions, a hyperbolic system of conservation laws has the form

$$\frac{\partial U}{\partial t} + \frac{\partial F}{\partial x} + \frac{\partial G}{\partial y} = 0 \ , \tag{7.1}$$

where for the inviscid gasdynamics equations

$$U = \begin{bmatrix} \rho \\ m \\ n \\ e \end{bmatrix} \ , \quad F = \begin{bmatrix} \rho u \\ \rho u^2 + p \\ \rho uv \\ u(e+p) \end{bmatrix} \ , \quad G = \begin{bmatrix} \rho v \\ \rho uv \\ \rho v^2 + p \\ v(e+p) \end{bmatrix} \ , \tag{7.2}$$

where $m = \rho u$, and $n = \rho v$. The primitive variables of (7.2) are density ρ, velocity components u and v, pressure p, and total energy per unit volume e. The equation of state is

$$p = (\gamma - 1)\left[e - \frac{1}{2}\left(\frac{m^2}{\rho} + \frac{n^2}{\rho}\right)\right] \tag{7.3}$$

This system can be rewritten in quasi-linear form as

$$\frac{\partial U}{\partial t} + A\,\frac{\partial U}{\partial x} + B\,\frac{\partial U}{\partial y} = 0\ , \tag{7.4}$$

where A and B are the Jacobian matrices

$$A = \partial F/\partial U\ , \qquad B = \partial G/\partial U\ , \tag{7.5a,b}$$

As in the previous section, we use the fact that $F(U)$ and $G(U)$ are homogeneous functions of degree one in U and consequently

$$F = AU\ , \qquad G = BU\ . \tag{7.6a,b}$$

For the inviscid equations of gasdynamics, the matrices A and B can be diagonalized as

$$Q^{-1}AQ = \begin{bmatrix} u & & & \\ & u & & 0 \\ & & u+c & \\ & 0 & & u-c \end{bmatrix} \qquad (k_1 = 1,\ k_2 = 0) \tag{7.7}$$

$$Q^{-1}BQ = \begin{bmatrix} v & & & \\ & v & & 0 \\ & & v+c & \\ & 0 & & v-c \end{bmatrix} \qquad (k_1 = 0,\ k_2 = 1) \tag{7.8}$$

where c is the local speed of sound. The matrices Q and Q^{-1}, as defined in Appendix B, are functions of the two parameters k_1, k_2 and of the dependent variables. The values of (k_1, k_2) indicated in the parentheses of (7.7) and (7.8) are the values

that diagonalize A and B. Since A and B do not commute, they cannot be diagonalized by the same similarity transformation.

The flux vectors F(U) and G(U) for the inviscid equations of gasdynamics can be split into subvectors, each of which depends on eigenvalues of the same sign exactly as in the one-dimensional case. A generalized flux vector

$$\mathscr{F}_{II} = Q\Lambda Q^{-1}U \ , \tag{7.9}$$

analogous to (4.19) for one space dimension, is given in Appendix B for two space dimensions. (For completeness, a three-dimensional version is also given.) By using the generalized flux vector, one can compute $F^{\pm}$, $G^{\pm}$ for any desired eigenvalue splitting. For example,

$$F^{+} = \mathscr{F}_{II}(k_1 = 1,\ k_2 = 0,\ \lambda_1^{+},\ \lambda_3^{+},\ \lambda_4^{+}) \tag{7.10}$$

where $\mathscr{F}_{II}$ as given by Eq. (B9) of Appendix B is evaluated using the particular values of the parameters (k_1,k_2) and $(\lambda_1,\ \lambda_3,\ \lambda_4)$ indicated in the parentheses of Eq. (7.10). The positive eigenvalues $\lambda_1^{+},\ \lambda_3^{+},\ \lambda_4^{+}$ are defined by Eq. (4.4), where $\lambda_1 = u$, $\lambda_3 = u + c$, $\lambda_4 = u - c$.

8. ALGORITHMS FOR TWO SPACE DIMENSIONS

Just as in the one-dimensional case, the split subvector forms allow construction of novel numerical difference schemes.

Explicit Methods

The natural extension of the upwind scheme (5.4), (5.5) to two spatial dimensions is

$$\overline{U^{n+1}_{j,k}} = U^n_{j,k} - \nu_x\left[\Delta_x(F^-_{j,k})^n + \nabla_x(F^+_{j,k})^n\right] - \nu_y\left[\Delta_y(G^-_{j,k})^n + \nabla_y(G^+_{j,k})^n\right] \tag{8.1}$$

$$\begin{aligned} U^{n+1}_{j,k} = \frac{1}{2}\Bigg\{ & U^{n+1}_{j,k} + U^n_{j,k} - \nu_x\left[\Delta_x(F^-_{j,k})^{\overline{n+1}} + \nabla_x(F^+_{j,k})^{\overline{n+1}}\right] \\ & - \nu_y\left[\Delta_y(G^-_{j,k})^{\overline{n+1}} + \nabla_y(G^+_{j,k})^{\overline{n+1}}\right] - \nu_x\left[\nabla^2_x(F^+_{j,k})^n - \Delta^2_x(F^-_{j,k})^n\right] \\ & - \nu_y\left[\nabla^2_y(G^+_{j,k})^n - \Delta^2_y(G^-_{j,k})^n\right]\Bigg\}, \end{aligned} \tag{8.2}$$

where $x = j\Delta x$, $y = k\Delta y$, and $\nu_x = \Delta t/\Delta x$, $\nu_y = \Delta t/\Delta y$. Although this upwind version of MacCormack's scheme requires considerably more work than the conventional scheme, it is a more robust algorithm if the solution exhibits large spatial gradients. In addition, as in the one-dimensional case, a very effective algorithm is obtained when the upwind scheme is alternated with the conventional MacCormack scheme on successive time steps.

If only first-order time accuracy is required, a simple explicit scheme is given by

$$U^{n+1}_{j,k} = U^n_{j,k} - \Delta t(\delta^b_x F^+ + \delta^f_x F^- + \delta^b_y G^+ + \delta^f_y G^-)\big|^n_{j,k}, \tag{8.3}$$

where δ^b and δ^f are defined by (5.8) and (5.9). Such a scheme is practical for steady state problems and it could be the basis of a point relaxation algorithm.

Implicit Methods

The natural extension of (5.7) to two spatial dimensions is

$$\left[I + \frac{\theta\Delta t}{1+\xi}\left(\nabla_x A^+_{j,k}|^n + \Delta_x A^-_{j,k}|^n + \nabla_y B^+_{j,k}|^n + \Delta_y B^-_{j,k}|^n\right)\right]\Delta U^n_{j,k}$$

$$= -\left(\frac{\Delta t}{1+\xi}\right)\left(\delta^b_x F^+_{j,k}|^n + \delta^f_x F^-_{j,k}|^n + \delta^b_y G^+_{j,k}|^n + \delta^f_y G^-_{j,k}|^n\right) + \left(\frac{\xi}{1+\xi}\right)\Delta U^{n-1}_{j,k} \ . \tag{8.4}$$

The left-hand side of the scheme (8.4) can be factored into the product of two operators as

$$\left[I + h\left(\nabla_x A^+_{j,k}|^n + \nabla_y B^+_{j,k}|^n\right)\right]\left[I + h\left(\Delta_x A^-_{j,k}|^n + \Delta_y B^-_{j,k}|^n\right)\right]\Delta U^n_{j,k} = \text{RHS (8.4)} \ ,$$

where

$$h = \frac{\theta\Delta t}{1+\xi} \tag{8.5}$$

and "RHS (8.4)" denotes the right-hand side of (8.4). This scheme can be implemented by the sequence

$$\left[I + h\left(\nabla_x A^+_{j,k}|^n + \nabla_y B^+_{j,k}|^n\right)\right]\Delta U^*_{j,k} = \text{RHS (8.4)} \ , \tag{8.6a}$$

$$\left[I + h\left(\Delta_x A^-_{j,k}|^n + \Delta_y B^-_{j,k}|^n\right)\right]\Delta U^n_{j,k} = \Delta U^*_{j,k} \ , \tag{8.6b}$$

$$U^{n+1}_{j,k} = U^n_{j,k} + \Delta U^n_{j,k} . \tag{8.6c}$$

Compared to the class of centrally-differenced implicit schemes [2, 14, 15] the algorithm (8.6) has both advantages and disadvantages. Equation (8.6a) requires the solution of a sparse block lower diagonal matrix and Eq. (8.6b) requires the solution of a sparse block upper bidiagonal matrix. Consequently, the computational inversion work is much less than that of solving two

block tridiagonal matrix sequences, as a conventional central-differenced algorithm would require. Moreover, in three dimensions the plus-minus split subvectors can still be approximately factored into just two factors — a sparse upper block-triangular matrix and a sparse lower block-triangular matrix. In three dimensions, the use of central spatial differences requires the inversion of three block tridiagonal sequences. The upwind differences are also dissipative, so it is not necessary to add higher-order dissipation terms.

On the other hand, twice as many Jacobian matrices and flux vectors have to be formed with the plus-minus splitting. Furthermore, these are more involved to form than the usual Jacobians, although with careful programming certain terms in $A^{\pm}$ and $B^{\pm}$ as well as $F^{\pm}$ and $G^{\pm}$ can be formed simultaneously.

Other difference schemes can be formulated that use the plus-minus flux vector splitting. An implicit second-order accurate scheme is given by

$$\left[I + h\left(\nabla_x A^{+}_{j,k}|^n + \Delta_y B^{-}_{j,k}|^n + \nabla_y B^{+}_{j,k}|^n\right)\right]\left[I + h\Delta_x A^{-}_{j,k}|^n\right]\Delta U^n_{j,k} = \text{RHS} \quad (8.4) \,. \tag{8.7}$$

This factorization does require a block tridiagonal inversion in the y-direction. Consequently, viscous terms in the y-direction can readily be included into the implicit operator.

A semi-implicit, first-order accurate scheme in time is obtained from Eq. (8.7) by dropping the factor $\left(I + h\Delta_x A^{-}_{j,k}|^n\right)$ and

letting $\theta = 1$, $\xi = 0$. Indeed, once the flux vectors are broken into subvectors, a large number of difference schemes can be devised to achieve possible advantages in numerical accuracy, robustness, computational efficiency, and storage.

9. NUMERICAL EXPERIMENTS IN TWO DIMENSIONS

Numerical calculations of model problems in two dimensions have been used to verify the stability and practicality of the algorithms of the last section. For example, the explicit algorithm (8.1) was tested on a square uniform grid with periodic boundary conditions. Waves were followed in time for arbitrary (non-physical) initial data. Although no results are shown, it was noted that the upwind scheme required about 3 times more computational time than standard MacCormack scheme.

The implicit algorithm (8.5), was tested on a simple biconvex airfoil with linearized boundary conditions. A typical transonic airfoil solution result is shown in Fig. 6 for a free-stream Mach number of 0.84 and a body thickness ratio of 11.4. The eigenvalue splitting (4.4) was used. Also shown are the calculated results obtained from the conventional implicit algorithm using central differencing. Both calculations use the same grid and boundary conditions. The grid is clustered in x and y and uses 50×28 points. The results shown are in good agreement for this coarse grid.

The numerical calculations illustrated two weaknesses of the upwind scheme that have now been essentially corrected. Whenever an eigenvalue changes sign, it is either suddenly set to zero or is suddenly nonzero. Elements of any one subvector are suddenly changed and the local accuracy of the difference approximation can suffer. In Fig. 6 one notices a small oscillation in the data at the sonic line where the (u - c) eigenvalue changes sign. This oscillation would actually appear much worse if it were not for the blending terms that are added to the eigenvalues to smooth out sudden changes. An example of blended terms are the following:

$$\lambda_1^+ = \frac{u + |u|}{2} + \varepsilon_1 \qquad \lambda_1^- = \frac{u - |u|}{2} - \varepsilon_1$$

$$\lambda_3^+ = \frac{u + c + |u + c|}{2} + \varepsilon_3 \qquad \lambda_3^- = \frac{u + c - |u + c|}{2} - \varepsilon_3$$

$$\lambda_4^+ = \frac{u - c + |u - c|}{2} + \varepsilon_4 \qquad \lambda_4^- = \frac{u - c - |u - c|}{2} - \varepsilon_4 \ ,$$

where ε_ℓ are small positive numbers which smoothly approach zero as $|\lambda_\ell|$ increases. We remark that nonconservative formulations are not afflicted with flux vectors that have discontinuous derivatives.

As previously noted, $A^+ \neq \partial F^+/\partial U$, although the two matrices share eigenvalues of the same sign. For the shock-tube calculations the time step was limited by accuracy considerations and no difficulty was encountered in using A^+ and A^- on the left-hand side of the implicit algorithm. In the steady state airfoil calculation we did find that using $A^\pm$ instead of $\partial F^\pm/\partial U$ imposed

explicit-like time-step restrictions. Use of the true Jacobian resulted in a more robust algorithm. This is quite a different result than was found with convection-sound speed splittings [3] in which the similarity matrix had identical stability properties to the actual Jacobian.

10. GENERAL CONSERVATION FORMS FOR HYPERBOLIC SYSTEMS

The implicit algorithms developed in the previous sections were for a Cartesian coordinate system; however, computational fluid dynamical problems involve flows over (or through) arbitrarily shaped bodies.

In this section we show that the previously derived algorithms can be made applicable to general flow fields. One method of handling complex geometries is to map the physical plane — for example, an airfoil in two spatial dimensions — into a rectangular computational plane. The desired transformation has the property that the airfoil surface is coincident with coordinate lines in the physical plane, and the airfoil surface lies along the boundary of the rectangular computational plane. The transform should also cluster grid points to regions where large spatial gradients occur. Since the actual numerical computation is carried out in a transformed rectangular plane with a uniform mesh, we review in this section the form of the transformed conservation-law equations and the corresponding difference algorithm.

It can be shown [16] that the conservation-law form (7.1) is retained under an arbitrary time-dependent coordinate transformation

$$\xi = \xi(x,y,t) \ , \qquad \eta = \eta(x,y,t) \ , \qquad \tau = t \ . \tag{10.1}$$

In particular, one obtains

$$\frac{\partial \hat{U}}{\partial \tau} + \frac{\partial \hat{F}}{\partial \xi} + \frac{\partial \hat{G}}{\partial \eta} = 0 \ , \tag{10.2}$$

where $\hat{U} = U/J$ and the flux vectors $\hat{F}$ and $\hat{G}$ are linear combinations of the vectors of (7.2):

$$\hat{F} = (\xi_t U + \xi_x F + \xi_y G)/J \tag{10.3a}$$

$$\hat{G} = (\eta_t U + \eta_x F + \eta_y G)/J \tag{10.3b}$$

and

$$J = \frac{\partial(\xi,\eta)}{\partial(x,y)} = \xi_x \eta_y - \xi_y \eta_x \tag{10.4}$$

is the Jacobian of the transformation. It is important to note that Cartesian components of velocity and momentum are retained in (10.2). The equations in three spatial dimensions are straightforward generalizations of the above equations.

As in the previous sections, we use the fact that $F(U)$ and $G(U)$ are homogeneous functions of degree one in U. As a consequence

$$\frac{F(U)}{J} = F(U/J) = F(\hat{U}) = A\hat{U} \ , \tag{10.5a}$$

$$\frac{G(U)}{J} = G(U/J) = G(\hat{U}) = B\hat{U} \ , \tag{10.5b}$$

where

$$A = \partial F(\hat{U})/\partial \hat{U} \ , \qquad B = \partial G(\hat{U})/\partial \hat{U} \ .$$

(Note that A and B are the Jacobians for Cartesian coordinates defined by Eq. (7.5).)

Hence, Eqs. (10.3) can be rewritten as

$$\left.\begin{aligned} \hat{F} &= (k_{10}I + k_{11}A + k_{12}B)\hat{U} \ , \\ \hat{G} &= (k_{20}I + k_{21}A + k_{22}B)\hat{U} \ , \end{aligned}\right\} \tag{10.6}$$

where $k_{10} = \xi_t$, etc., are the scale factors. The generalized flux vector $\mathcal{F}_{II}$ defined in the appendix can be used to calculate $\hat{F}^{\pm}$, $\hat{G}^{\pm}$ for any arbitrary eigenvalue splitting. This is apparent from Eqs. (B7), (B6), and (B1) of Appendix B because the coefficients k_1 and k_2 of Eq. (B1) are arbitrary real numbers, which for the present application are taken to be the scale factors ξ_t, ξ_x, ξ_y, etc. Finally, since the conservation-law form is retained by (10.2), the numerical algorithms of Sec. 7 are directly applicable to general conservation forms.

11. CONCLUDING REMARKS

A hyperbolic system of conservation laws whose associated Jacobian matrices have positive and negative eigenvalues can only be spatially differenced as a system with centered operators. However, splitting the flux vectors into subvectors whose associated eigenvalues are of the same sign allows use of one-sided (upwind) operators.

In this paper, we have made use of the fact that flux vectors of the inviscid gasdynamic equations are homogeneous functions of

degree one to construct flux vector splittings. As a consequence, new explicit and implicit dissipative difference methods are devised which are more robust and computationally efficient than conventional spatially centered schemes. Preliminary computational experiments show that the new methods are feasible, although clearly both additional analysis and numerical testing on "realistic" problems are required.

APPENDIX A: INSTABILITY OF ONE-SIDED SCHEMES FOR HYPERBOLIC SYSTEMS WITH EIGENVALUES OF MIXED SIGN

Here we examine the hyperbolic system of equations

$$\frac{\partial U}{\partial t} + A \frac{\partial U}{\partial x} = 0 \ , \tag{A1}$$

where A is a constant matrix with both positive and negative eigenvalues. In Sec. 2 it was shown that approximating $\partial_x U$ with either $\nabla_x U$ or $\Delta_x U$ must always lead to instability for the time-continuous system of equations. In this Appendix, we argue that all conventional backward, forward, or biased (e.g., Eq. (2.13)) finite-difference approximations to $\partial_x U$ will be unstable if A has both positive and negative eigenvalues.

As shown in Sec. 2, Eq. (A1) can be transformed into an uncoupled system of scalar wave equations of the form

$$\frac{\partial u}{\partial t} + \lambda \frac{\partial u}{\partial x} = 0 \ , \tag{A2}$$

where λ is either positive or negative. With introduction of a spatial-difference approximation, Eq. (A2) is replaced by a system of ordinary differential equations

$$\frac{d\vec{u}}{dt} = M\vec{u} + \vec{f} \,, \tag{A3}$$

where $\vec{u} = (u, u_2, u_3, \ldots, u_j, \ldots)^t$, $u_j \simeq u(j\Delta x)$, $\vec{f}$ contains known boundary data (if any) and M is a constant coefficient matrix. For example, if ∂_x is approximated by ∇_x with given boundary data on the left-hand boundary, then

$$M = -\frac{\lambda}{\Delta x}\begin{bmatrix} 1 & & & & & \\ -1 & 1 & & & & \\ & -1 & 1 & & & \\ & & -1 & 1 & & \\ & & & \ddots & \ddots & \\ & & & & -1 & 1 \end{bmatrix}, \quad \vec{f} = \frac{\lambda}{\Delta x}\begin{bmatrix} u_o \\ 0 \\ 0 \\ 0 \\ \vdots \\ \vdots \\ \vdots \end{bmatrix} . \tag{A4}$$

If ∂_x is approximated by Eq. (2.13), then

$$M = -\frac{\lambda}{6\Delta x}\begin{bmatrix} -3 & 6 & -1 & & & \\ -2 & -3 & 6 & -1 & & \\ & -2 & -3 & 6 & -1 & \\ & & \ddots & \ddots & \ddots & \ddots \\ & & & \ddots & \ddots & \ddots \end{bmatrix}, \quad \vec{f} = \frac{\lambda}{6\Delta x}\begin{bmatrix} 2u_o \\ 0 \\ 0 \\ 0 \\ \vdots \\ \vdots \\ \vdots \end{bmatrix} . \tag{A5}$$

In this latter example the values of M would change to accommodate an alternative choice of differencing at the right-hand boundary.

The solution of Eq. (A3) is (cf. [17, 18])

$$\vec{u} = e^{Mt}\,\vec{u}_o + \text{particular solution} .$$

If M has an eigenvalue with a positive real part, then $e^{Mt} \to \infty$ as $t \to \infty$ and the solution is unbounded. However, any conventional backward, forward, or biased differenced scheme leads to a matrix M with a nonzero real trace. The trace contains λ as a multiplier and the sum of the eigenvalues of M equals its trace. Consequently, for either the case λ positive or λ negative, $e^{Mt} \to \infty$ as $t \to \infty$ since at least one eigenvalue will have a positive real part. Thus, conventional backward, forward, or biased difference schemes are unstable.

The above argument, showing instability, is not altered by boundary conditions since they will only affect a few end-point elements of the matrix M. For a large matrix (refined spatial grid), these few elements cannot alter the sign of the trace. Note that the use of central spatial differencing, which can be stable, leads to a matrix M with zero trace. We remark also that a non-conventional upwind differencing such as

$$\left.\frac{\partial u}{\partial x}\right|_j \simeq \frac{u_{j-1} - u_{j-2}}{\Delta x} ,$$

also has a zero trace and thus must be proved to be unstable by another argument.

APPENDIX B: GENERALIZED FLUX VECTOR FOR TWO AND THREE SPATIAL DIMENSIONS

Two-Dimensional Case

The system of conservation laws (7.1) can be rewritten in quasi-linear form (7.4). Define a matrix P as

$$P = k_1 A + k_2 B \ , \tag{B1}$$

where k_1 and k_2 are arbitrary real numbers. The system (7.4) is hyperbolic at the point (x, y, t, U) if there exists a similarity transformation such that

$$Q^{-1}PQ = \begin{bmatrix} \lambda_1 & & & 0 \\ & \lambda_2 & & \\ & & \lambda_3 & \\ & & & \ddots \\ 0 & & & \lambda_m \end{bmatrix} = \Lambda \ , \tag{B2}$$

where the eigenvalues λ_ℓ are real and the norms of Q and Q^{-1} are uniformly bounded.

The formulas in the remainder of this appendix pertain to the inviscid equations of gasdynamics for a perfect gas. The Jacobians A and B are 4×4 matrices and Q and Q^{-1} can be written as

$$Q = MT \ , \qquad Q^{-1} = T^{-1}M^{-1} \ , \tag{B3}$$

where M, T, and their inverses are given in the appendix of [2]. In general, the elements of Q and Q^{-1} are functions of the parameters (k_1, k_2) and the dependent variables. For example, the elements $(Q)_{33}$ and $(Q^{-1})_{33}$ are

$$Q_{33} = \frac{\rho}{\sqrt{2}c}(v + c\tilde{k}_2) , \qquad (Q^{-1})_{33} = \frac{1}{\sqrt{2}\rho c}[c\tilde{k}_1 - (\gamma - 1)u] ,$$

where u and v are the x- and y-velocity components, ρ is the density, c is the local speed of sound, γ is the ratio of specific heats, and

$$\tilde{k}_1 = k_1/(k_1^2 + k_2^2)^{1/2} , \qquad \tilde{k}_2 = k_2/(k_1^2 + k_2^2)^{1/2} . \tag{B4}$$

The eigenvalues λ_ℓ of P are

$$\left.\begin{aligned} \lambda_1 = \lambda_2 = k_1u + k_2v , \qquad \lambda_3 = \lambda_1 + c(k_1^2 + k_2^2)^{1/2} , \\ \lambda_4 = \lambda_1 - c(k_1^2 + k_2^2)^{1/2} . \end{aligned}\right\} \tag{B5}$$

Formula (B2) can be rewritten as

$$P = k_1A + k_2B = Q\Lambda Q^{-1} . \tag{B6}$$

Hence, the matrix A or B, or any linear combination, can be recovered from (B6).

As in the one-dimensional case (see Sec. 4), it is convenient to define a generalized flux vector by

$$\mathcal{F}_{II} = Q\hat{\Lambda}Q^{-1}U , \tag{B7}$$

where now the eigenvalues $\hat{\lambda}_\ell$ of the diagonal matrix $\hat{\Lambda}$ are taken to be arbitrary. Although the matrix Q^{-1} is rather complex, the product $Q^{-1}U$ is simply

$$Q^{-1}U = \begin{bmatrix} \dfrac{\rho(\gamma - 1)}{\gamma} \\ 0 \\ \dfrac{c}{\sqrt{2}\gamma} \\ \dfrac{c}{\sqrt{2}\gamma} \end{bmatrix} . \tag{B8}$$

Completing the computation for the generalized flux vector we obtain

$$\mathcal{F}_{II} = \frac{\rho}{2\gamma}\begin{bmatrix} 2(\gamma-1)\hat{\lambda}_1 + \hat{\lambda}_3 + \hat{\lambda}_4 \\ 2(\gamma-1)\hat{\lambda}_1 u + \hat{\lambda}_3(u + c\tilde{k}_1) + \hat{\lambda}_4(u - c\tilde{k}_1) \\ 2(\gamma-1)\hat{\lambda}_1 v + \hat{\lambda}_3(v + c\tilde{k}_2) + \hat{\lambda}_4(v - c\tilde{k}_2) \\ (\gamma-1)\hat{\lambda}_1(u^2+v^2) + \frac{\hat{\lambda}_3}{2}[(u+c\tilde{k}_1)^2 + (v+c\tilde{k}_2)^2] \\ \quad + \frac{\hat{\lambda}_4}{2}[(u-c\tilde{k}_1)^2 + (v-c\tilde{k}_2)^2] + W_{II} \end{bmatrix} \tag{B9}$$

where

$$W_{II} = \frac{(3-\gamma)(\hat{\lambda}_3 + \hat{\lambda}_4)c^2}{2(\gamma-1)}$$

and $\tilde{k}_1$, $\tilde{k}_2$ are defined by Eq. (B4). The conventional flux vector F(U) is obtained from (B9) if $k_1 = 1$, $k_2 = 0$, and the λ_ℓ's as given by (B5) are inserted in (B9). Likewise, G(U) is recovered if $k_1 = 0$, $k_2 = 1$. Formula (B9) can be used to obtain any flux vector splitting as described in Secs. 7 and 10.

Three-Dimensional Case

In three spatial dimensions, a hyperbolic system of conservation laws has the form

$$\frac{\partial U}{\partial t} + \frac{\partial F(U)}{\partial x} + \frac{\partial G(U)}{\partial y} + \frac{\partial H(U)}{\partial z} = 0 . \tag{B10}$$

This system can be rewritten in quasi-linear form as

$$\frac{\partial U}{\partial t} + A\frac{\partial U}{\partial x} + B\frac{\partial U}{\partial y} + C\frac{\partial U}{\partial z} = 0 , \tag{B11}$$

where A, B, C are the Jacobian matrices

$$A = \frac{\partial F}{\partial U} , \qquad B = \frac{\partial G}{\partial U} , \qquad C = \frac{\partial H}{\partial U} . \tag{B12}$$

The generalization of (B1) is

$$P = k_1 A + k_2 B + k_3 C . \tag{B13}$$

The eigenvalues of P are

$$\left.\begin{aligned} \lambda_1 = \lambda_2 = \lambda_3 &= k_1 u + k_2 v + k_3 w , \\ \lambda_4 = \lambda_1 + c(k\cdot k)^{1/2}, \quad \lambda_5 &= \lambda_1 - c(k\cdot k)^{1/2}, \end{aligned}\right\} \tag{B14}$$

where

$$k\cdot k = k_1^2 + k_2^2 + k_3^2 .$$

The matrices M, T, and their inverses, which are needed to compute Q and Q^{-1} as defined by Eq. (B3), are given in [6]. The generalized flux vector for three space dimensions is defined by

$$\mathscr{F}_{III} = Q\hat{\Lambda}Q^{-1}U , \tag{B15}$$

where the eigenvalues $\hat{\lambda}_\ell$ of the 5×5 diagonal matrix $\hat{\Lambda}$ are again arbitrary. For the purpose of calculating $\mathscr{F}_{III}$, we assume that $\hat{\lambda}_1 = \hat{\lambda}_2 = \hat{\lambda}_3$ because this is the case for the physical eigenvalues of the matrix P defined by Eq. (B14) and for the eigenvalue splittings of interest. The product $Q^{-1}U$ is

$$Q^{-1}U = \frac{1}{\gamma}\begin{bmatrix} \rho k_1(\gamma - 1) \\ \rho k_2(\gamma - 1) \\ \rho k_3(\gamma - 1) \\ c/\sqrt{2} \\ c/\sqrt{2} \end{bmatrix} \tag{B16}$$

and the generalized flux vector is

$$\mathcal{F}_{III} =$$

$$\frac{\rho}{2\gamma}\begin{bmatrix} 2(\gamma-1)\hat{\lambda}_1 + \hat{\lambda}_4 + \hat{\lambda}_5 \\ \hline 2(\gamma-1)\hat{\lambda}_1 u + \hat{\lambda}_4(u+c\tilde{k}_1) + \hat{\lambda}_5(u-c\tilde{k}_1) \\ \hline 2(\gamma-1)\hat{\lambda}_1 v + \hat{\lambda}_4(v+c\tilde{k}_2) + \hat{\lambda}_5(v-c\tilde{k}_2) \\ \hline 2(\gamma-1)\hat{\lambda}_1 w + \hat{\lambda}_4(w+c\tilde{k}_3) + \hat{\lambda}_5(w-c\tilde{k}_3) \\ \hline (\gamma-1)\hat{\lambda}_1(u^2+v^2+w^2) + \frac{\hat{\lambda}_4}{2}[(u+c\tilde{k}_1)^2 + (v+c\tilde{k}_2)^2 + (w+c\tilde{k}_3)^2] \\ + \frac{\hat{\lambda}_5}{2}[(u-c\tilde{k}_1)^2 + (v-c\tilde{k}_2)^2 + (w-c\tilde{k}_3)^2] + W_{III} + P \end{bmatrix} \tag{B17}$$

where

$$W_{III} = \frac{(3-\gamma)(\hat{\lambda}_4 + \hat{\lambda}_5)c^2}{2(\gamma-1)}$$

$$P = 2\rho(\gamma-1)\hat{\lambda}_1\tilde{k}_1(\tilde{k}_2 w - \tilde{k}_3 v) ,$$

u, v, and w are the x-, y-, and z-velocity components, and

$$\tilde{k}_1 = k_1/(k_1^2 + k_2^2 + k_3^2)^{1/2} , \quad \tilde{k}_2 = k_2/(k_1^2 + k_2^2 + k_3^2)^{1/2}$$

$$\tilde{k}_3 = k_3/(k_1^2 + k_2^2 + k_3^2)^{1/2} .$$

REFERENCES

1. R. F. WARMING AND R. M. BEAM, Upwind second-order difference schemes and applications in aerodynamic flows, AIAA J. 14 (1976), 1241.
2. R. F. WARMING AND R. M. BEAM, On the construction and application of implicit factored schemes for conservation laws, Symposium on Computational Fluid Dynamics, New York, April 16-17, 1977, SIAM-AMS Proceedings, 11 (1978), 85.
3. J. L. STEGER, Coefficient matrices for implicit finite difference solution of the inviscid fluid conservation law equations, Computer Methods in Applied Mechanics and Engineering 13 (1978), 175.
4. G. MORETTI, An old integration scheme for compressible flows revisited, refurbished and put to work, AE Report No. 78-22, Polytechnic Institute of New York, 1978.
5. R. COURANT, "Differential and Integral Calculus," Vol. II, Interscience, New York, 1936.
6. R. F. WARMING, R. M. BEAM, AND B. J. HYETT, Diagonalization and simultaneous symmetrization of the gas-dynamic matrices, Math. Comp. 29 (1975), 1037.
7. L. B. SCHIFF AND J. L. STEGER, Numerical simulation of steady supersonic viscous flow, AIAA Paper 79-0130, New Orleans, La., 1979.

8. R. W. MacCORMACK, The effect of viscosity in hypervelocity impact cratering, AIAA Paper 69-354, Cincinnati, Ohio, 1969.

9. J. E. FROMM, A numerical study of buoyancy driven flows in room enclosures, Lecture Notes in Physics, Vol. 8, pp. 120-126, Springer-Verlag, Berlin, 1971.

10. R. M. BEAM AND R. F. WARMING, An implicit factored scheme for the compressible Navier-Stokes equations II: The numerical ODE connection, AIAA Paper 79-1446, Williamsburg, Va., 1979.

11. H. W. LIEPMANN AND A. ROSHKO, "Elements of Gasdynamics," John Wiley & Sons, New York, 1957.

12. R. W. MacCORMACK AND B. S. BALDWIN, A numerical method for solving the Navier-Stokes equations with application to shock-boundary layer interactions, AIAA Paper 75-1, Pasadena, Calif., 1975.

13. R. M. BEAM AND R. F. WARMING, An implicit factored scheme for the compressible Navier-Stokes equations, AIAA J. 16 (1978), 393.

14. J. L. STEGER, Implicit finite difference simulation of flow about arbitrary two-dimensional geometries, AIAA J. 16 (1978), 679.

15. R. M. BEAM AND R. F. WARMING, An implicit finite-difference algorithm for hyperbolic systems in conservation-law form, J. Comput. Physics 22 (1976), 87.

16. H. VIVIAND, Formes conservatives des equations de la dynamique des gaz, La Recherche Aerosp., No. 1974-1, 1974, pp. 65-66.

17. G. STRANG, "Linear Algebra and Its Applications," Academic Press, New York, 1976.

18. F. R. GANTMACHER, "The Theory of Matrices," Vol. I, Chelsea Publishing Co., New York, 1959.

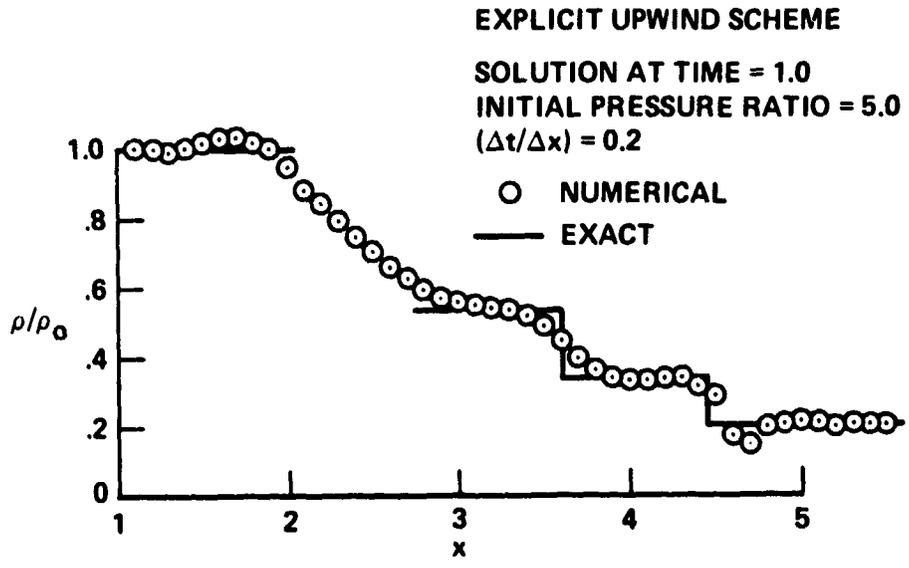

FIG. 1. Shock-tube solution obtained using explicit upwind scheme.

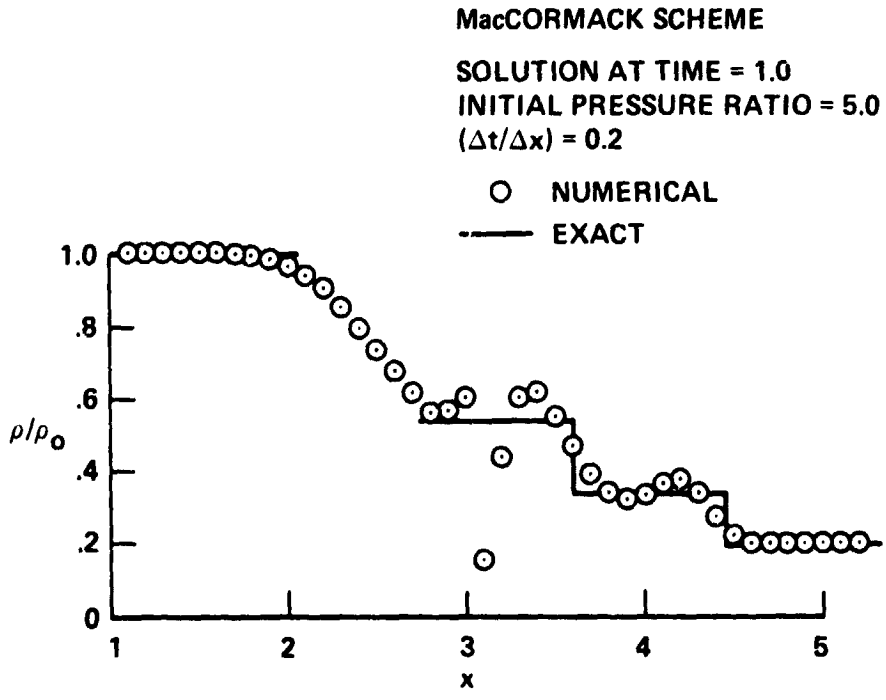

FIG. 2. Shock-tube solution obtained with explicit MacCormack scheme.

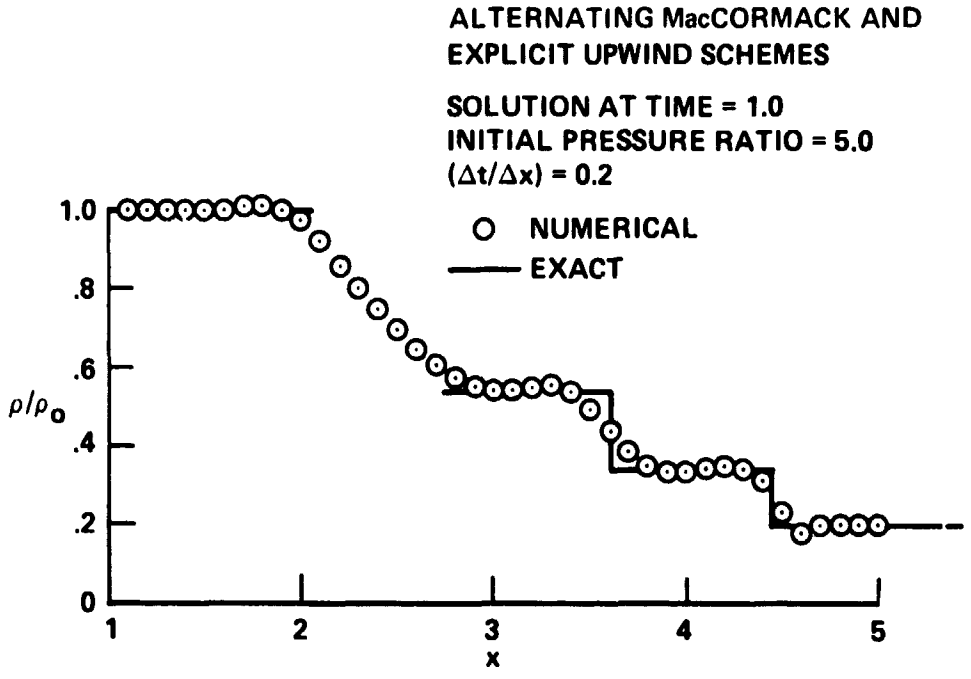

FIG. 3. Shock-tube solution obtained by alternating explicit upwind and MacCormack schemes.

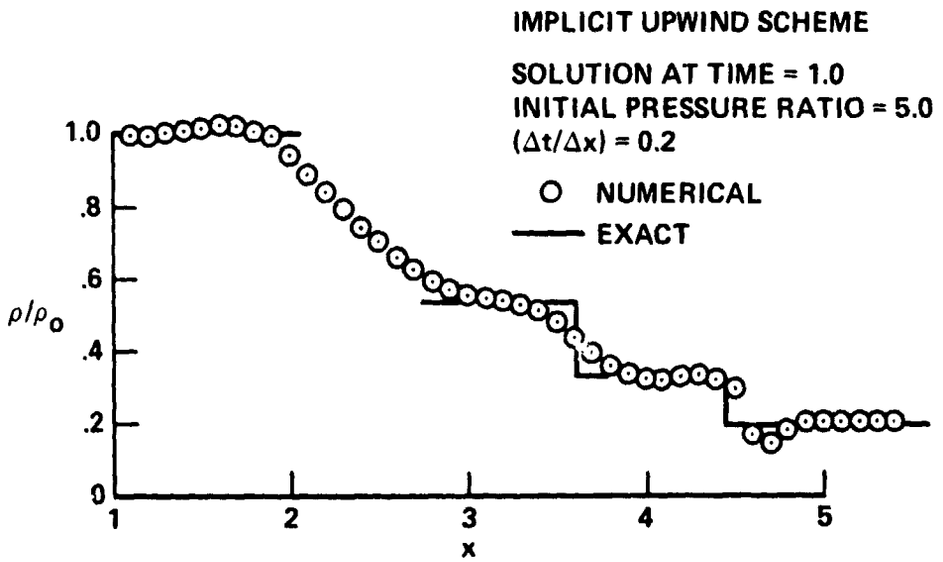

FIG. 4. Shock-tube solution obtained from implicit upwind scheme.

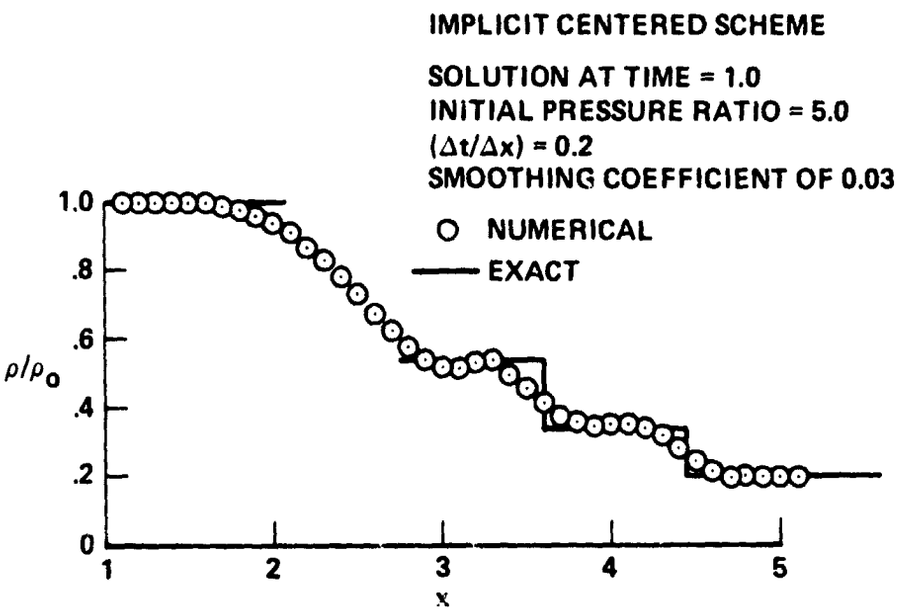

FIG. 5. Shock-tube solution obtained using implicit algorithm with central spatial differencing.

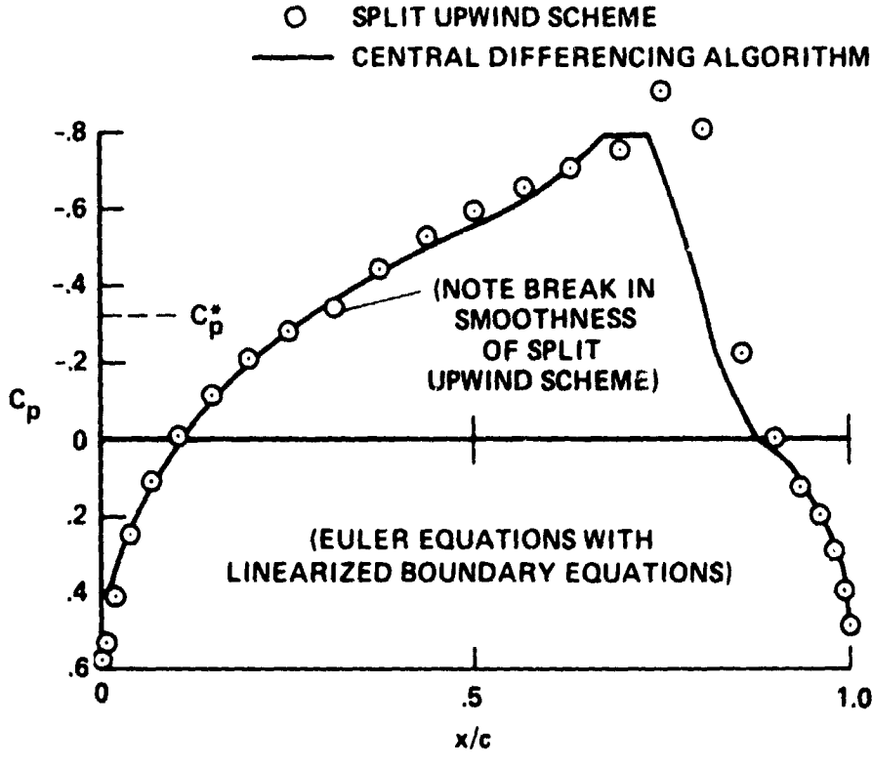

FIG. 6. Steady state solution for 11.4% thick parabolic arc airfoil, $M_\infty = 0.84$.

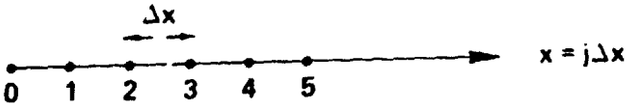

F.G. 7. One-dimensional grid.